Porous Media for Reentry Applications

Georges Duffa
CEA

France

gduffa@club-internet.fr

ABSTRACT

For re-entry highly porous carbon phenolic materials have known an important development in the recent past. We give first a short description of these materials. Then we describe their physico-chemical behavior focusing on specific problems induced by this porosity on creation of gases, composition and permeation of these gases, energy coupling between gas and solid and radiative problems. An section is devoted to experiments which are problematic for this kind of material. For each part an analysis of different possible approximations is given. The conclusion suggest some possible works to improve the modeling of these phenomena.

Contents

1.0 INTRODUCTION

During a long time a re-entry material was a black box endowed with some properties measured in dedicated laboratories. This approach was justified by the use of overall approximate models. Even efficient this method has proved its limits with the development of modern modeling permitting to access the mesoscopic scales presents in materials and associated phenomena with possible different scales. The approach has moved toward a more detailed description at macroscopic level permitted by the computational possibilities and a better knowledge of mesoscopic level corresponding to the scales defined by the material and, in some case, by scales induced by coupling with the flow [1]. This paper presents some progress made in the description of pyrolysis of carbon phenolic materials. But these detailed description brings out some new problems, some of them being open today.
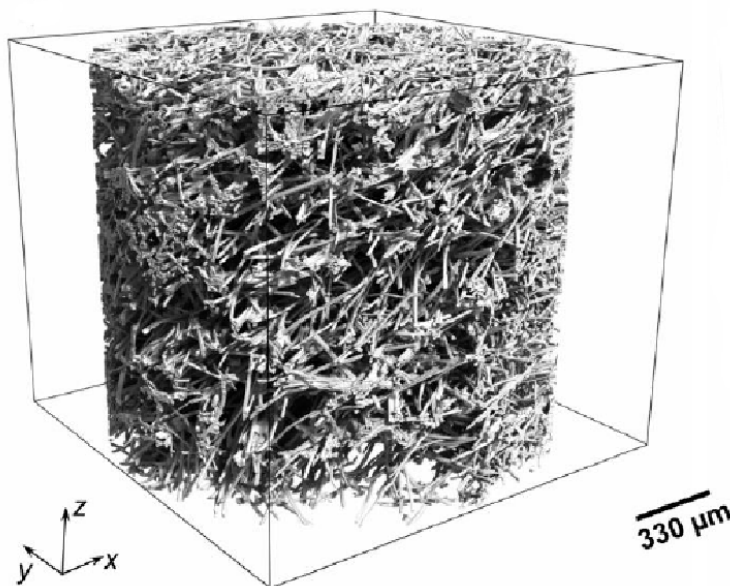
2.0 CARBON PHENOLICS

Figure 1: *Short fibers carbon phenolic material microtomography* [2].

More of the materials used for medium-to-high heat fluxes reentries are carbon phenolics. Tape Wrapped Carbon Phenolics (TWCP) are dense materials ($\rho \simeq 1450 \ kg \cdot m^{-1}$) used for Pioneer, Galileo and Hayabusa probes but also for booster nozzles. This kind of material is constituted of draped 2D weaved yarns (except in singular points like stagnation region of probes), each yarn being constituted by an ensemble of some hundred long fibers. More recently lightweight materials ($\rho < 400 \ kg \cdot m^{-1}$) have been developed for medium or moderately high fluxes. They use a carbon preform made of short fibers more or less randomly put together. An example is given in figure 1. In both cases the carbon assembly is filled with a resin.
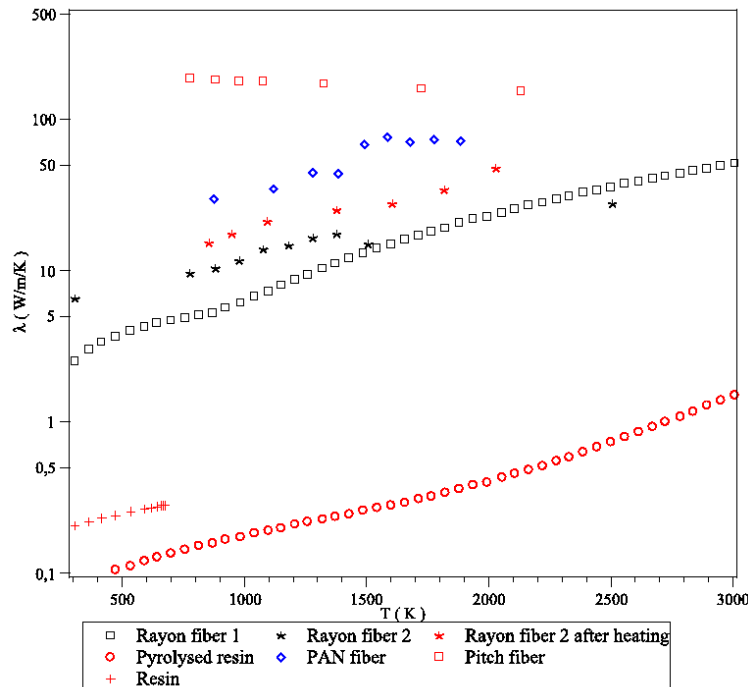
2.1 Fibers

Figure 2: *Fibers and resin conductivities* [3–5]. The values for charred resin were obtained by identification of measurements on a TWCP and are imprecise.

Even if different fibers are available all these materials were made with rayon fibers used for their low conductivity despite their low mechanical properties. These fibers have an irregular section with a mean diameter form 7 to $15 \mu m$.

The density vary between 1400 and 2000 $kg \cdot m^{-3}$ [3, 6].

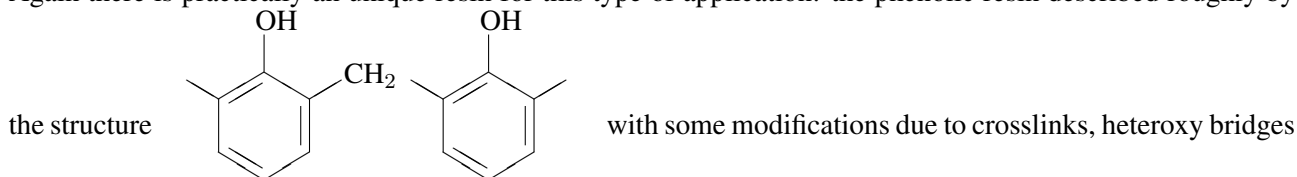The transversal conductivity of these fibers is lower due to their structural organization.

The conductivities of different fibers is given in Figure 2. We see

- The conductivity depends of thermal treatment applied by the manufacturer during fabrication $(1500 - 2500 \, K)$ and then varies from a fiber to another.

- A consequence of previous comment is the fact that the conductivity is not exactly the same during the temperature rising and the cooling phase, due to structural modifications which happens for temperatures higher than the temperature treatment. Note that this structural modification is endothermic and modify also slightly the heat capacity at low temperature.

- The conductivity significantly increases with temperature.

- The values of rayon fiber conductivity is much less than polyacrylonitrile (PAN) or pitch fibers.

2.2 Resin

Again there is practically an unique resin for this type of application: the phenolic resin described roughly by

the structure [chemical structure: two phenol rings with OH groups and CH₃ substituents connected by a CH_2 bridge] with some modifications due to crosslinks, heteroxy bridges

$(-H_2 - O - CH_2-)$, substitution of an $-H$ by CH_2OH, presence of nitrogen, *et cætera*. Some impure resins contains inorganic residues. The structure contains a polar bond -OH able to stick water molecules.

The density is about $1270 \ kg \cdot m^{-3}$ and the heat of formation $\Delta H^0_{f_{298}} = -1.0 \ MJ \cdot kg^{-1}$ [1].

2.3 Water

The third element seldom mentioned is the water absorbed by both other components. This phenomenon is a reversible process.

Rayon fibers have an important nanoporosity and can absorb up to 15% moisture in mass. The resin absorb up to 4%. The mechanisms of absorption-desorbtion is described in [1], Appendix F. This water have important effects when present during heating [7]. For re-entry applications the long stay in space makes this problem non-existent.

3.0 PYROLYSIS OF RESIN

3.1 Thermal decomposition

Temperature (K)	Reaction	Type
$600 < T < 800$	$R_{CH_2} \rightarrow R(CH_3)_n$	depolymerization
	$2R_{CH_2} \rightarrow R_{CH} + H_2O$	condensation $(-CH_2-) + (-OH)$
$700 < T < 1100$	$2R_{CH_2} \rightarrow R_O + H_2O$	condensation $(-OH) + (-OH)$
	$R_O \rightarrow R + O$	
	$R_{CH_2} + O \rightarrow R + CO + H_2$	
	$R_{CH_2} + H_2O \rightarrow R + CO + 2H_2$	reaction $(-CH_2-) + H_2O$
	$R_{CH_2} + H_2 \rightarrow R + CH_4$	reaction $(-CH_2-) + H_2$
	$R_{CH} \rightarrow R + H_2$	
$T > 900$	$R \rightarrow R_d + H_2$	deshydrogenation

Table 1: *Pyrolysis reactions for quasi-static heating. R is a benzenic cycle. $R(CH_3)_n$ means phenol, cresol, xylenol, etc. R_X stand for a bond of aromatic cores by X. R is a direct bond between aromatic cores and R_d two sticked cores (graphene). Nitrogen is omitted ($C_6H_5NH_2$, NH_3). This scheme is close to Trick's description* [8].
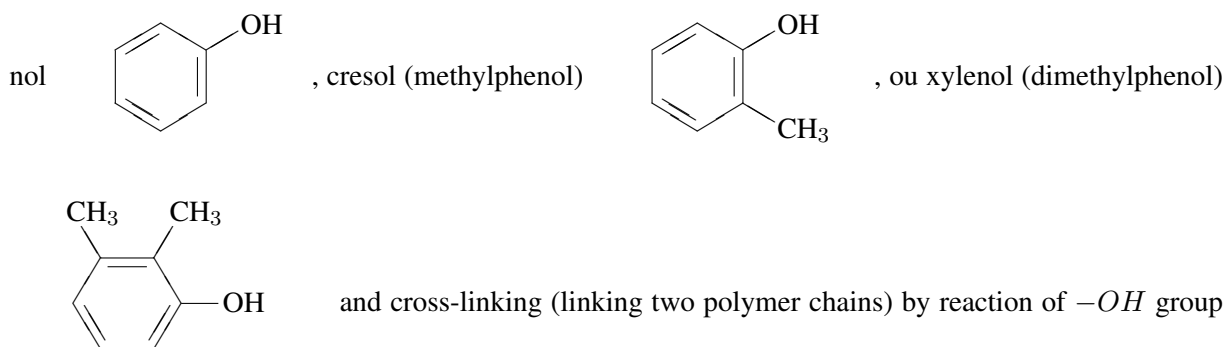
Note first that the gases formed during pyrolysis are driven to the surface and that, consequently, the decomposition takes place in an atmosphere formed by the pyrolysis gases themselves in the absence of any other component from the atmosphere. The experiments we use are conducted in a neutral atmosphere, on samples

R_{CH_2}	$\rightarrow$	$R_2 \ + \ 0.5 \, H_2O \ + \ 0.5 \, R(CH_3)_n$
R_2	$\rightarrow$	$R \ + \ 0.13 \, H_2O \ + \ 0.13 \, CO \ + \ 0.15 \, CH_4 \ + \ 0.59 \, H_2$
R	$\rightarrow$	$R_d \ + \ H_2$

Table 2: *Global reaction system. R_2 is a go-between R_{CH_2} and R_{CH} in proportion to the mass loss data. The description of gas produced are given by Sykes* [9].

previously dried. We can distinguish [8] three sets of reactions (temperatures quoted correspond to experiments carried out at very slow rise in temperature), identified by infrared spectrometry of the gases formed:

- between $600 \ K$ and $800 \ K$, two reactions leading to the depolymerization: creation of monomers phe-

nol , cresol (methylphenol) , ou xylenol (dimethylphenol)

 and cross-linking (linking two polymer chains) by reaction of $-OH$ group

  with a methylene bridge $(-CH_2-)$ and formation of H_2O,

- between $700 \ K$ and $1100 \ K$ condensation occurs by binding $-OH$ with $-CH_2-$, and a series of gas-solid reaction leading to the production of H_2, CO and CH_4 (table 1),

- between $900 \ K$ and $1200 \ K$ there is essentially a dehydrogenation, which produces of a more or less graphitized carbon.

However, the chemical evolution can not fully describe what is happening. Indeed, beyond $1600 \ K$, it is observed [10] a significant decrease in porosity resulting from the rearrangement of carbon at nano-level.

One can give the production of gas for each group of reactions from the reactions (Figure 2) and the laws of mass loss as defined below. An example is shown in Figure 3. It is only approximate values since each of the reactions contained in a group do not occur exactly at the same time. We note that there are significant differences between authors in the respective amounts of gases produced [8, 9].

3.2 Mass loss

The laws describing the mass loss is obtained by performing experiments made with fast pyrolysis temperature increases of up to $100 \ K \cdot s^{-1}$ or more. One should be wary of the very high heating rates that do not necessarily need the necessary quasi-constant temperature of the sample. These experiments highlight the major reactive groups described above. We observe a strong shift of the peaks with the rate of temperature rise, due to an activation energy.
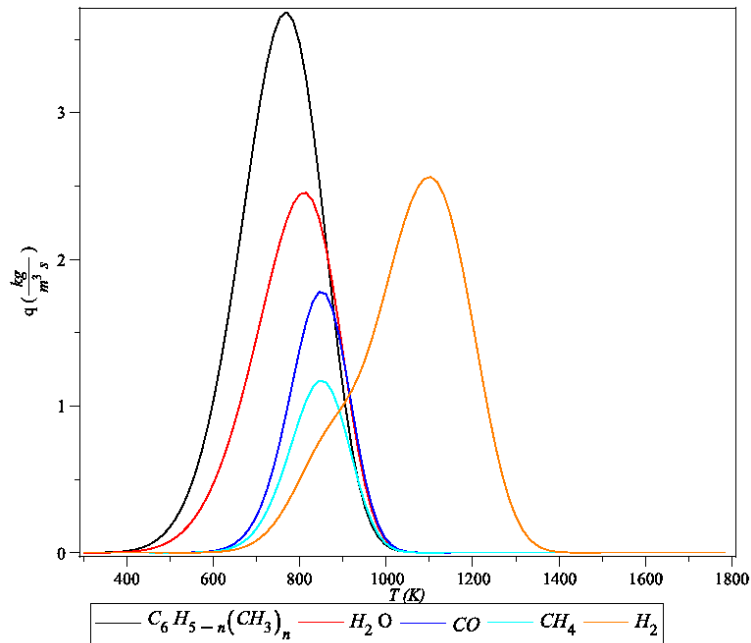
Figure 3: *Production of pyrolysis gases for a temperature rise of $1.67\ K \cdot s^{-1}$ [9]. Note discrepancies with table 1.*

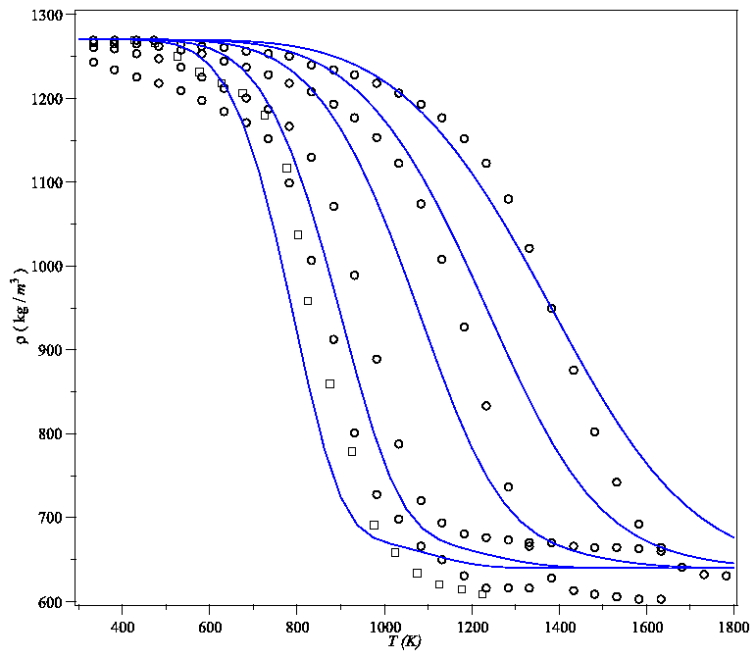**Figure 4:** *Mass loss for different temperature rising speeds ($0.17, 5, 20, 50$ et $100\ K \cdot s^{-1}$). The first experimental steps corresponds probably to water desorption.*

The description of the reactions is in principle similar to that of a gas mixture. The molar mass of solid compounds is unknown (large), it is included in the reaction constants. Many of these constants correspond to

irreversible reactions and therefore the backward reaction constants are assumed zero. However this method is not usable due to lack of data. Modelling is usually done in a limited framework where we ignore the effect of gas present and where it is assumed irreversible reactions of order n_i. A species is described by its partial density ρ_i and g_{ij}, defined as the mass fraction of this species transformed in species j during its pyrolysis (we assume that there may be competing reactions). The true densities of the intermediate solid products of pyrolysis are difficult to measure. It is assumed that they have the same density as resin. The pleasant consequence of this hypothesis is that there exist a bijective relation between density and porosity.

The ρ_i will be described, in a homogeneous medium, by the following differential system

$$\frac{d\rho_i}{dt} = \dot{\omega}_{s_i} = -k_i \rho_i^{n_i} + \sum_{\substack{j=1 \\ j \neq i}}^{n_e} g_{ji} k_j \rho_j^{n_j} \qquad i = 1, n_e \tag{1}$$

The reaction constants are usually expressed by an Arrhenius law

$$k_j = A_j \, exp\left(-\frac{T_{a_j}}{T}\right) \tag{2}$$

One can not in general give a relation for $\frac{d\rho}{dt}$, except when it is assumed (most of the time implicitly) direct (no competitive reactions) and independent reactions: the reaction $n + 1$ begins when the nth is complete. Supposing a one-step mechanism the system is described simply by

$$\frac{d\rho_R}{dt} = -k(\rho_R - \rho_C)^n \tag{3}$$

ρ_C is the density of final species (char). Taking into account $\rho = \rho_R + \rho_F$ (ρ_F being the density of fibers) we have the same relation for total density of material

$$\frac{d\rho}{dt} = -k(\rho - \rho_f)^n \tag{4}$$

The gas created is supposed leaving the surrounding solid phase with a negligible velocity.

3.3   Char

The final product is a glassy carbon accounting for about 50% of the initial mass of resin. Its conductivity is very low (see Figure 2) and its influence on radiative absorption low as can be seen on differences between PICA and pyrolyzed PICA [11].

4.0   GAS FLOW

4.1   Thermodynamic gas state

The Figure 5 illustrate the thermodynamic state of the gas when flowing through porosity. Just after their creation these gases are driven to the surface. In the first instant the temperature rise $v\frac{dT}{dx}$ is not sufficient to permit the chemical reactions to be efficient. Up to $\simeq 1200K$ in the example the medium is frozen. After that chemical reactions takes place and reaches equilibrium at high temperatures: $\simeq 2500K$ in our example. Most of the models uses a one-step pyrolysis reaction conducting to a constant mass fraction of gases. This hypothesis is not true in general due to the different steps of resin degradation and eventual carbon deposition during the migration of gases.

This observation conduct to the conclusion that chemical equilibrium is only an approximation and can induce errors in the low temperature regions of material.
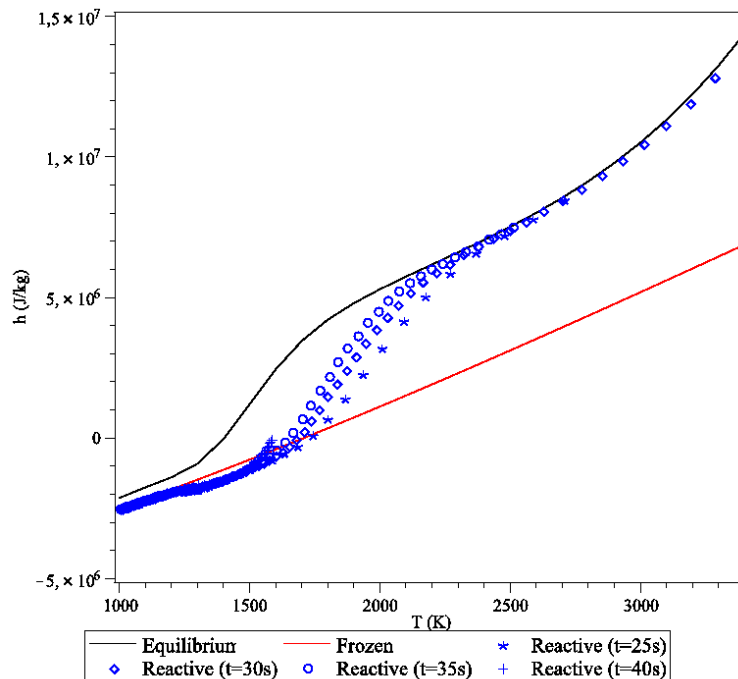
Figure 5: *Influence of the thermodynamic state of the pyrolysis gases (enthalpies). "Reactive" profiles correspond to a thermodynamic nonequilibrium calculation made in post-processing the example treated in [12, 13] at different times during re-entry.*

4.2 Chemical reactions

The problem of chemical gaseous reactions is analogous to the problem encountered in combustion. A great number of species are present in the medium as seen in Figure 6. In the first part of re-entry when the surface is at low temperature a great number of species including high molar weight species are injected in the boundary layer. This problem was never treated to the knowledge of the author. At higher temperatures the problem becomes more tractable the species reaching the surface being limited to H_2, H, CO, C_2H_2, C_3H_3 (more than 1% in volume) and to less extend C_2H, CH_3, CH_4, C_3. Note that this description correspond only to the example treated. Other species can be present, for example NH_3 and CN, depending on the resin composition and temperature gradient in the material [14]. A detailed mechanism is proposed in [15]. The problem of reduction of kinetic mechanisms is persistent in combustion and some methods developed to face the difficulty [16].

4.3 Carbon formation from gases

Solid carbonaceous products can be created from the pyrolysis gases. Almost all materials exhibits the presence of deposited carbon on the internal surface. Even in very small quantities it can be detected by X-ray analysis. Its importance is low for low density carbon phenolics. The mechanisms of formation is treated in [1]. Note that these mechanisms conduct also to the formation of soots probably present in low (negligible?) quantities.
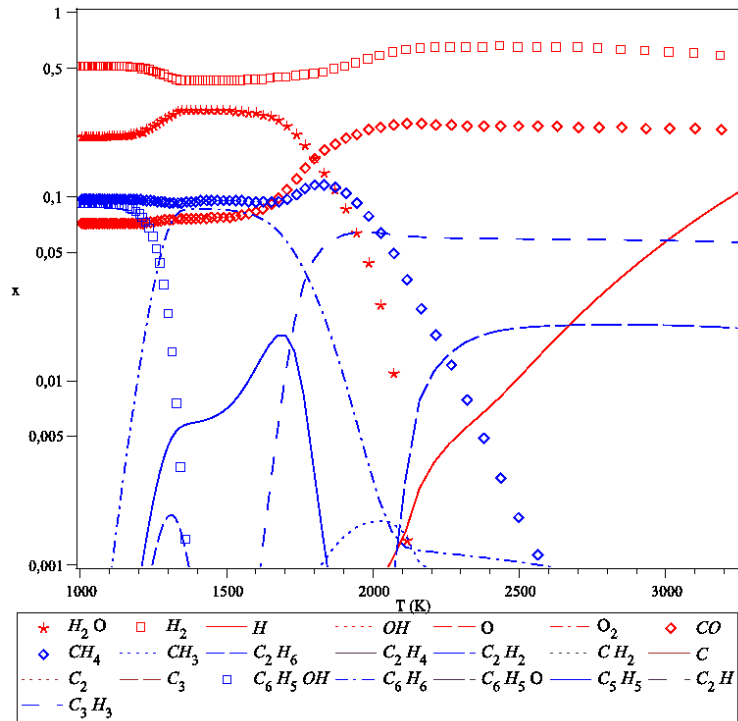
Figure 6: *Nonequilibrium pyrolysis gas corresponding to Figure 5 (t=30s).*

4.4 Gas flow description

4.4.1 Conservation equations

Generally the medium is supposed continuous. This is not really true near the surface at high temperature where the mean free path is some microns long. This effect is weak in the core of material. The modeling of this kind of flow is given in [17, 18]. Continuity equation describe

- gas mass

$$\frac{\partial(\epsilon\rho_{g_i})}{\partial t} + \nabla \cdot (\epsilon\rho_{g_i}\mathbf{v}) = \epsilon\dot{\omega}_{g_i} + S_V \dot{m}_{g_i} \tag{5}$$

where ϵ is the porosity, $\dot{\omega}_{g_i}$ the mass creation by unit volume from gases and $\dot{m}_{g_i}$ the mass creation by unit surface on the volume surface S_V.

Integrating on all species we obtain

$$\frac{\partial(\epsilon\rho_g)}{\partial t} + \nabla \cdot (\epsilon\rho_g\mathbf{v}) = \epsilon\dot{\omega}_g + S_V \dot{m}_g \tag{6}$$

In thermodynamic equilibrium $\dot{\omega}_g = 0$.

- total energy (one-temperature medium)

$$\frac{\partial(\rho E)}{\partial t} + \nabla \cdot (\dot{q}_s + \dot{q}_{rad}) + \nabla \cdot [\epsilon(\rho_g h_g \mathbf{v} + \dot{q}_g)] = 0 \tag{7}$$

$\dot{q}_s$ and $\dot{q}_{rad}$ contains the porosity. The gas conduction $\dot{q}_g$ is generally negligible compare to the convective term.

The volume total energy ρE is given by

$$\rho E = \sum_i \rho_{s_i} e_{s_i} + \epsilon \left(\sum_i \rho_{g_i} h_{g_i} + \frac{\rho_g v^2}{2} \right) \tag{8}$$

The last term of this equation is negligible [13]. The first term is globalized in $\rho_s e_s = \sum_i \rho_{s_i} e_{s_i}$. This term is measured or calculated from mixture law.

In the case of thermal nonequilibrium of the two phases one should write two equations with a coupling term $H_V (T_g - T_s)$.

4.4.2 Simplified equations

In the past a popular simplified system was used supposing

- a one-dimensional problem,

- an instantaneous outgassing. Then the mass flow rate then writes

$$\dot{m}_g = \epsilon \rho_g v = -\int_{-\infty}^{y} \frac{\partial \rho}{\partial t} dy' \tag{9}$$

- in the total energy the part of the gas is neglected then $E = e_s$. Conduction in the gas is also neglected $\dot{q}_g = 0$.

- one-step pyrolysis.

With these approximations we can write

1.

$$\begin{aligned} \nabla \cdot (\epsilon \rho_g h_g \mathbf{v}) &= h_g \nabla \cdot (\epsilon \rho_g \mathbf{v}) + \epsilon \rho_g \mathbf{v} \cdot \nabla h_g \\ &= h_g \nabla \cdot (\dot{m}_g \tfrac{\mathbf{v}}{v}) + \dot{m}_g C_{p_g} \tfrac{\mathbf{v}}{v} \cdot \nabla T \end{aligned} \tag{10}$$

with

$$\rho_g C_{p_g} = \sum_i \rho_{g_i} C_{p_{g_i}} + \sum_i h_{g_i} \frac{\partial \rho_{g_i}}{\partial T} \tag{11}$$

2.

$$h_g \nabla \cdot (\dot{m}_g \frac{\mathbf{v}}{v}) = h_g \frac{\partial \dot{m}_g}{\partial y} = -h_g \frac{\partial \rho}{\partial t} \tag{12}$$

3.

$$\begin{aligned} \tfrac{\partial}{\partial t}(\rho_s e_s) &= \tfrac{\partial}{\partial t}(\sum_i \rho_{s_i} e_{s_i}) \\ &= \left[\sum_i \rho_{s_i} C_{V_{s_i}} + \sum_i e_{s_i} \frac{\partial \rho_{s_i}}{\partial T} \right] \frac{\partial T}{\partial t} \\ &= \left[\rho_s C_{V_s} + \sum_i e_{s_i} \frac{\partial \rho_{s_i}}{\partial T} \right] \frac{\partial T}{\partial t} \end{aligned} \tag{13}$$

4. We introduce the advancement rate

$$\xi = \frac{\rho_v - \rho}{\rho_v - \rho_C} \in [0, 1] \tag{14}$$

where ρ_v is the virgin density.

In the case of one-step reaction we have

$$\sum_i e_{s_i} \frac{\partial \rho_{s_i}}{\partial T} = \frac{(1 - \xi)\rho_v e_v + \xi \rho_C e_C}{\rho_v - \rho_C} \frac{\partial \rho}{\partial T} \tag{15}$$

Then the system reduce to an unique equation for energy plus a quadrature (equation 9)

$$\rho C_{V_s} \frac{\partial T}{\partial t} + \dot{m}_g C_{p_g} \frac{\partial \rho}{\partial y} + \Delta h_p \frac{\partial \rho}{\partial t} + \nabla \cdot (\dot{q}_s + \dot{q}_{rad}) = 0 \tag{16}$$

with

$$\Delta h_p = \frac{(1 - \xi)\rho_v e_v + \xi \rho_C e_C}{\rho_v - \rho_C} - h_g \tag{17}$$

This last quantity is sometimes globalized as "heat of degradation" characteristic of material and treated as an experimental constant value [19].

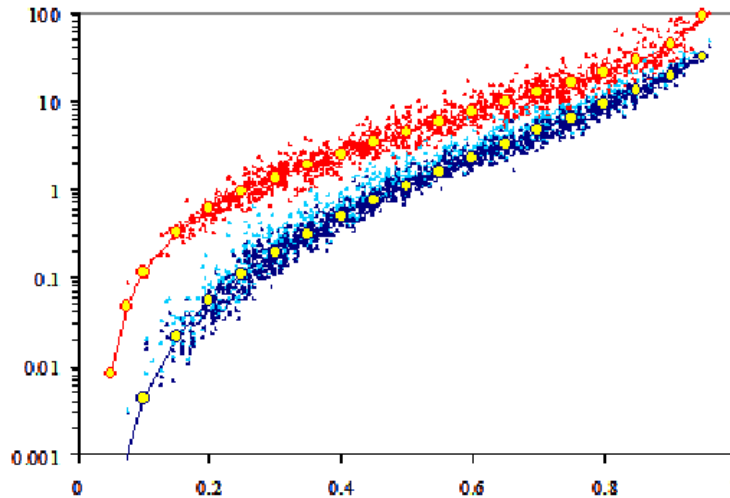### 4.4.3 Transport properties

Figure 7: *Relation diffusion coefficient with porosity on two material axes. Each point correspond to a calculation made from a small volume of the reconstituted carbon-carbon material.* [20].

Independently of the state of the gas the modeling of gas flow requires some information on momentum and energy exchanges with the solid. Generally the medium is supposed continuous. This is not really true near the surface at high temperature where the mean free path is some microns long. This effect is weak in the core of material. The transport properties of interest are

- conductivity in the solid,

- radiative properties: absorption and scattering,

- permeability K and Ergun number α which can have a small influence in our case [13]. These coefficients are present in the Darcy-Forchheimer equation

$$K\nabla p = -\mu\mathbf{v}(1 + \alpha\mathcal{R}_K) \tag{18}$$

where $\mathcal{R}_K$ is the Reynolds number calculated with the characteristic length $K^{\frac{1}{2}}$

$$\mathcal{R}_K = \frac{\rho v K^{\frac{1}{2}}}{\mu} \tag{19}$$

The Ergun number was measured on a pyrolyzed a nylon phenolic of porosity 0.8 [21]. The value of α was close to 0.15.

- heat transfer coefficient between gas and solid,

- eventually specific surface if one is interested in gas-solid reactions [22].

These quantities can be measured more or less precisely. For example permeability of PICA and its pre-form are available in [23, 24], apparent conductivity in [11], radiative properties in [25]. The acquisition of microtomography like that shown on Figure 1 offers an unique opportunity to evaluate all these quantities. An illustration of this method is given in Figure 7 for a carbon-carbon material at different steps of infiltration. The microtomography is treated to reconstitute the internal geometry and calcultions are made on different small volumes at different steps. After that a correlation is constructed to give a mean relation with porosity.

The descriptive equations of the gas-solid system are described in another paper of this Lecture [26].

4.4.4 Transport properties in the pyrolysing zone

It is almost impossible to measure the geometrical evolution of porosity during pyrolysis. The nature of material itself (the material formed from the resin) is not known (see Section 3.1). The necessity to know the transport properties during this phase conduct to use approximate methods based on the correlation of this property with a variable known from calculation, generally the porosity or the advancement rate.

An example is given in Figure 8 in which the conductivity of a carbon phenolic was calculated using different mean values corresponding to possible simple arrangements of media. The differences between results are not significative considering the precision of mass loss (see Figure 4).

Other methods exists based on physical approach on simple geometrical configurations. An example is the Ergun's method for the calculation of permeability and Ergun number in packed systems. Also exist some derived methods using the permeability to calculate the other parameter [13]. These methods gives only orders of magnitude.

4.4.5 Gas-solid equilibrium

We will focus on a problem poorly treated in the case of re-entry domain. This problem is associated to the difference of temperature between gas and solid. The phenomenon is presented in [26]. Measurements on materials of interest seems lacking. We can give an idea of order of magnitude using a study made on a silica phenolic with lower porosities (0.3 vs. 0.9 for PICA) and permeabilities (10^{-15} vs. $10^{-10}\ m^2$) for the pyrolysed material. The value of heat transfer coefficient from measurements was $H_V = 2 - 4 \times 10^5\ W \cdot m^{-3} \cdot K^{-1}$
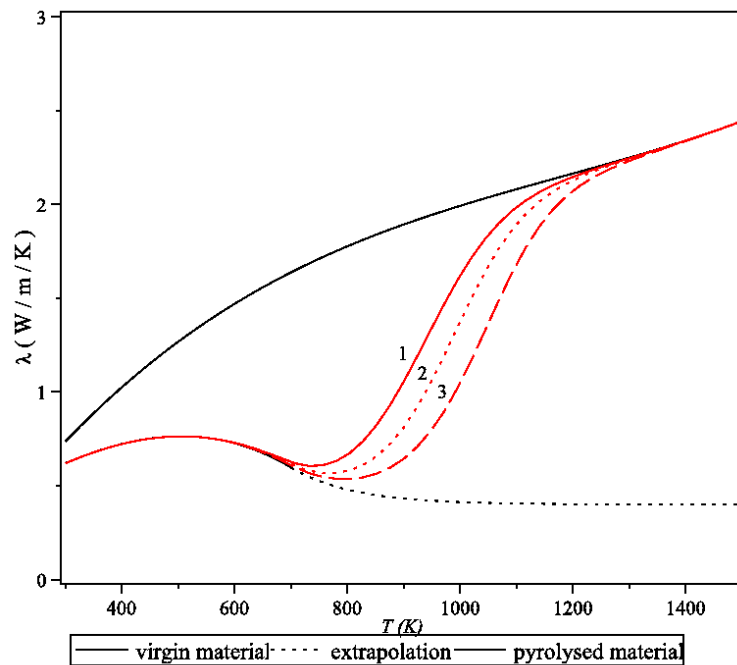
Figure 8: *TWCP carbon phenolic conductivity from virgin and pyrolyzed materials [27]: arithmetic mean (1), geometric mean (2) and harmonic mean (3). Pyrolysis at* $20\ K \cdot s^{-1}$.

using a correlation $Nu = \frac{H_v K}{\lambda_g} = a\mathcal{R}_K^b$ for the experiments [28]. On these materials a temperature gap of about $100\ K$ was calculated in moderate heatflux input conditions ($0.2\ MW \cdot m^{-2}$), conducting to a maximum surface temperature of $1200\ K$ [29]. The materials like PICA having higher porosity and permeability than those studied on can anticipate a lower value of the coupling coefficient. Some results on PICA-like carbon phenolic are parametrized in [15] in a more representative case conducting to surface temperature of $2000\ K$. The results are reproduced in Figure 9, suggesting temperature gap of some hundred K for realistic heat transfer coefficient. In this calculation the surface has an unique temperature of gas and solid, hypothesis to be discussed now.

We can separate the boundary surface in two parts:

- near the stagnation region the external velocity component parallel to the surface is negligible. The surface has a negligible effect on gas-solid flow and exchanges. Then there is no boundary condition for solid: its surface temperature is free.

- far from the stagnation point we face a rarefied Brinkman flow in which the external flow induces a velocity component under the surface up to depth comparable to mean length between fibers (some tens microns). This modification of internal flow enhance locally the coupling gas-solid. This problem was studied mainly for continuous incompressible flows [30]. To the knowledge of author the problem in our case is open.
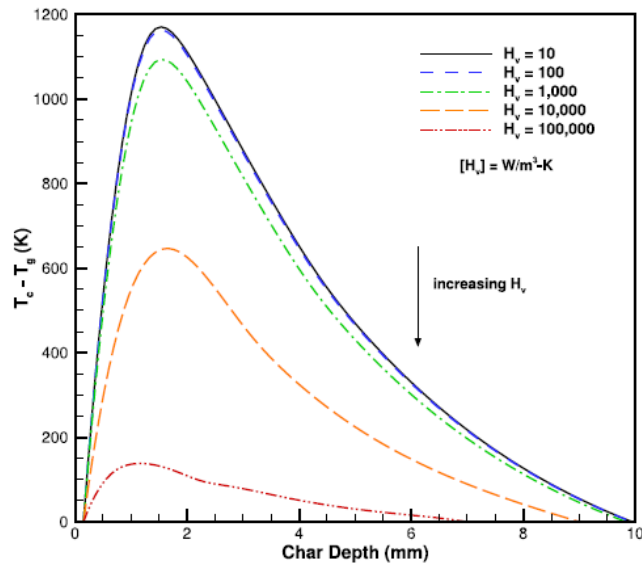
Figure 9: *Influence of volumetric heat transfer exchange [15].*

4.5 Experiments on these materials

The problem for testing porous materials is the dimension: the radius of sample is not negligible compare to the characteristic thickness of pyrolysis zone. The gas is permeating in any direction as seen on Figure 10, driven by surface pressure. This effect diminishes the pyrolysis efficiency and the blowing effect near stagnation point. Mass flow of pyrolysis gases can be lowered up to one order of magnitude at stagnation point [31].

In the case of a preform this kind of experiment conduct to an artefact where the surface gas in ingested by the material.

5.0 RADIATION IN MATERIAL

In PICA-like materials the radiative transfer play an important role as soon as $1000~K$ and becomes dominant for $T > 2000~K$. This can be seen on Figure 11 where the true conduction is compared to an equivalent conductivity supposing diffusion regime valid. These values were given by analytic calculation on a random assembly of fibers and char spheres and confirmed by experience [25, 32].

The radiative properties can be obtained by specific experiences [33] but also calculated from microtomographies using known surface properties as done in another paper of this Lecture [34].

Once obtained these properties the radiative transfer can be calculated by various methods. To show the problems we test the severe case of a constant heat flux of $9.2~MW \cdot m^{-2}$ on pyrolyzed PICA material with isotropic or anisotropic entering intensity (a ray). This example gives a thermal lenght $\frac{T}{|\nabla T|}$ of same order of magnitude than the mean free path in the material, say $130~\mu m$.

From the results on Figure 12 one can conclude

- for this case P_{13} and M_1 are sufficient to give a reasonable precision ($< 1\%$ on temperature) when compared to a reference calculation using S_{96}.

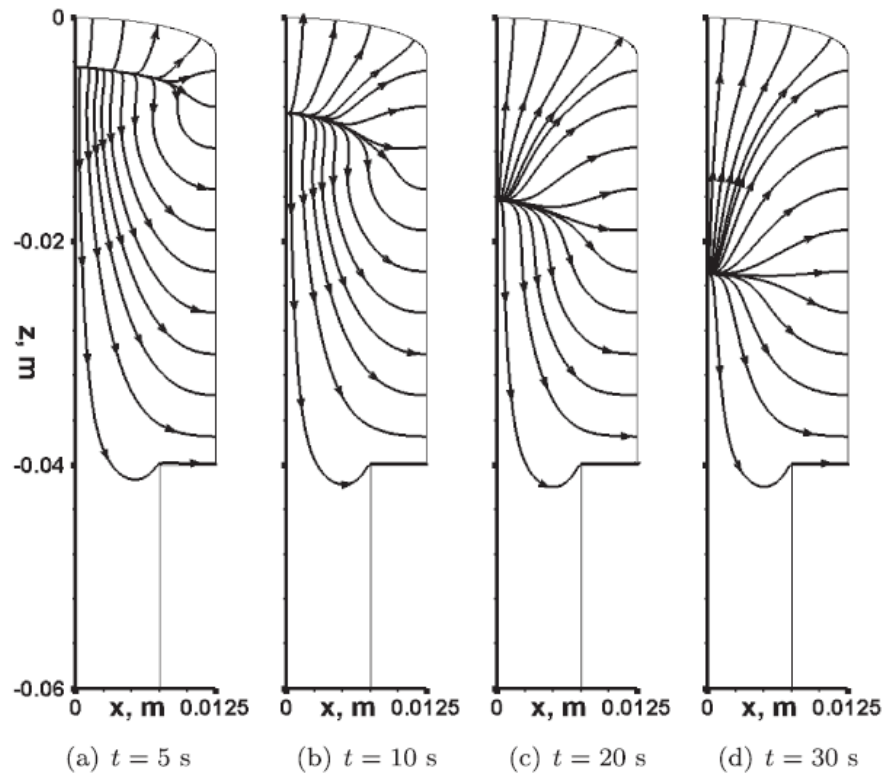(a) $t = 5$ s   (b) $t = 10$ s   (c) $t = 20$ s   (d) $t = 30$ s

Figure 10: *Plasma Jet experiment on a PICA specimen (typical geometry) [31].*

- the diffusion approximation gives an unacceptable result.

To see the origin of the problem when using equivalent conductivity the Eddington factor ($\frac{1}{3}$ for diffusion) was plotted on Figure 13. The discrepancy in the deep region is not important, corresponding to low temperatures are then to non-pyrolyzed material. But near surface one see the effect of semi-transparency, also visible on Figure 12. A non-negligible part of ingoing flux is directly deposited in material and a part of re-radiation comes from the interior of material. The consequence is a lower re-radiation compare to an opaque material.

The problem of diffusive calculation is not the approximation in the material itself but the boundary condition applied. The solution is to use a radiative solver or to write a new boundary condition, a difficult task!

CONCLUSION

In the different mechanisms involved in pyrolysis of hightly porous carbon phenolic materials some problems remains open:

- the pyrolysis of resin are generally imperfectly described and some uncertainty remains on gas created in the first stage of gasification.

- energy exchange between gas and solid in not known. The probable low exchange can have some influence on the response of material, particularly at surface where not taking into account the phenomenon
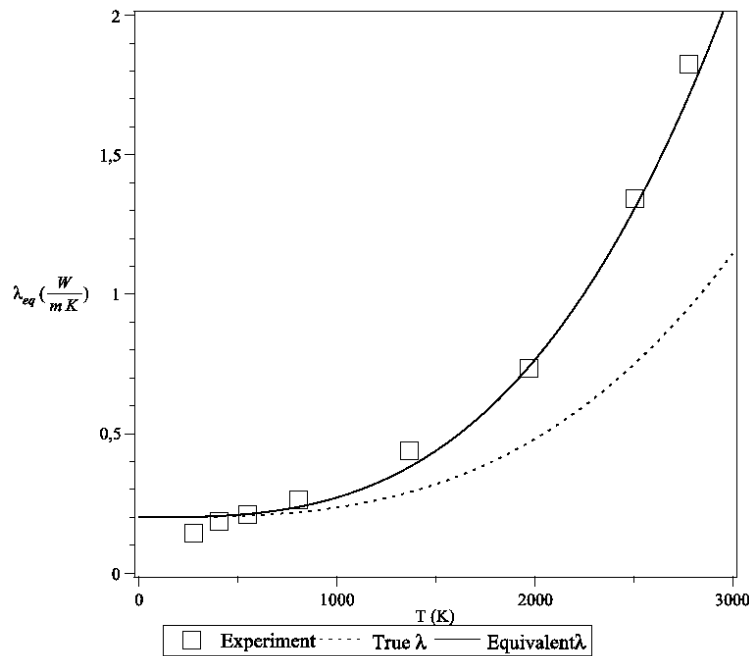
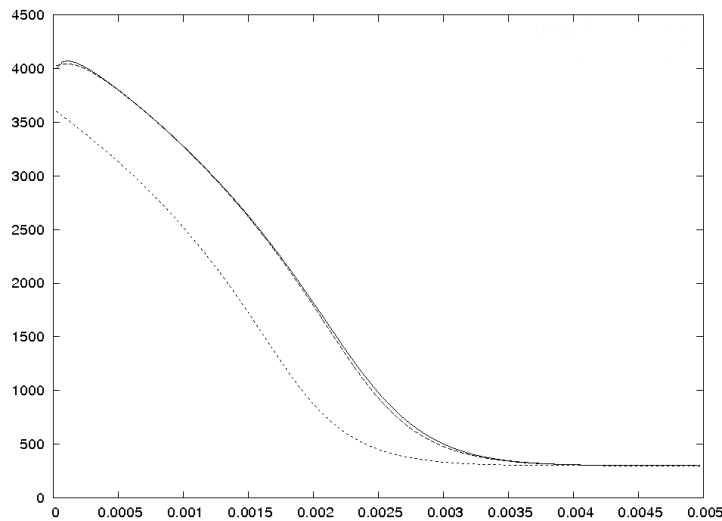**Figure 11:** *PICA conductive, radiative and total (apparent) conductivity [32].*

Figure 12: *Numerical test on pyrolysed PICA with an isotropic impidging radiation corresponding to a heat flux of $10\ MW \cdot m^{-2}$ at $t = 1\ s$. Temperatures in K vs. depth in m. The curves correspond to two radiative calculations (P_{13} and M_1 models) and an diffusive calculation.*

leads to an overvaluation of quality of material.

- the modeling of time-evolving transport properties is generally poor. Even if the consequences seems low when compared to other uncertainties, a progress in this matter would be welcome.

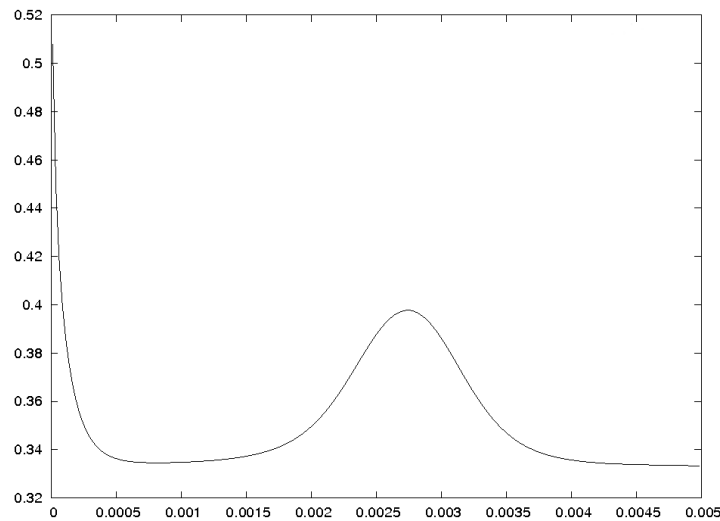- a progress will come from the use of tomographies.

Figure 13: *Eddington factor vs. depth (m). Anisotropic entering intensity.*

- in the case of severe re-entries a radiative problem exists at surface making the usual diffusion approximation inadequate and conducting also to an overvaluation of material quality.

- one must take great care in plasma jet testing where habitual geometries used for sample conduct to physical artefacts which, in this case, gives an undervaluation of material.

REFERENCES

[1] Duffa, G., *Ablative Thermal Protection Systems Modeling*, Education Series, AIAA, Reston, 2013.

[2] Panerai, F., Ferguson, J., Lachaud, J., Martin, A., Gash, M. J., and Mansour, N. N., "Analysis of Fibrous Felts for Flexible Ablators using Synchrotron Hard X-ray Micro-Tomography," 8th European Symposium on Aerothermodynamics for Space Vehicles, Lisbon, Portugal, March 2015.

[3] Pradere, C., Batsale, J., Goyhénèche, J., Pailler, R., and Dilhaire, S., "Thermal Properties of Carbon Fibers at Very High Temperature," *Carbon*, Vol. 47, No. 3, March 2009, pp. 737–743.

[4] Lagedrost, J. F., Fabish, T. J., Eldrige, E. A., Deem, H. W., Krause, H. H., and Vaughan, D. A., "Thermophysical and Chemical Characterization of Charring Ablative Materials," Tech. Rep. CR 73399, NASA, Dec. 1968.

[5] Clayton, W. A., Fabish, T. J., and Lagedrost, J. F., "Thermal Conductivity of Phenolic-Carbon Chars," Tech. Rep. TR-69-313, NASA, Dec. 1969.

[6] Savage, G., *Carbon-Carbon Composites*, Chapman et Hall, London, 1993.

[7] Vignoles, G., Gillant, A., Epherre, J.-F., Mosnier, P., and Dourges, A.-M., "First steps of the Degradation of a Carbon/Phenolic Composite: the Role of Moisture Transfer," 16th International Conference on Composites Materials, Kyoto, Japan, July 2007.

[8] Trick, K. A., *Reaction Kinetics of the Pyrolysis of Phenolic/Carbon Composite Material*, Ph.D. thesis, University of Dayton, Dayton, 1994.

[9] Sykes, G. F., "Decomposition Characteristics of a Char-Forming Phenolic Polymer used for Ablative Composites," Tech. Rep. TN D-3810, NASA, Feb. 1967.

[10] Ducamp, V., *Transferts thermiques dans un matériau composite carbone-résine*, Ph.D. thesis, Universit Bordeaux 1, Bordeaux, April 2002.

[11] Tran, H. K., Johnson, C. E., Rasky, D. J., Hui, F. C. L., HSU, M.-T., and Chen, Y. K., "Phenolic Impregnated Carbon Ablators (PICA) for Discovery Class Missions," *AIAA Paper 2010-1175*, 31th Thermophysics Conference, New Orleans, Louisiana, June 1996.

[12] Amar, A. J., Blackwell, B. F., and Edwards, J. R., "One-Dimensional Ablation with Pyrolysis Gas Flow Using Finite Control Volume Procedure," *AIAA Paper 2007-4535*, 39th AIAA Thermophysics Conference, Miami, Florida, June 2007.

[13] Martin, A. and Boyd, I., "Non-Darcian Behavior of Pyrolysis Gas in a Thermal Protection System," *Journal of Thermophysics and Heat Transfer*, Vol. 24, No. 1, March 2010, pp. 60–68.

[14] Martin, A. and Boyd, I., "Chemistry Model for Ablating Carbon-Phenolic Material during Atmospheric Re-entry," *AIAA Paper 2010-1175*, 48th AIAA Aerospace Sciences Meeting Including the New Horizons Forum and Aerospace Exposition, Orlando, Florida, Jan. 2010.

[15] Scoggins, J. B., *The Development of a Thermochemical Nonequilibrium Ablation and Pyrolysis Model for Carbon-Phenolic Thermal Protection Systems*, Master's thesis, North Carolina State University, Raleigh, 2011.

[16] Tomlin, A. S., Turanyi, T., and Pilling, M. J., *Mathematical Tools for the Construction, Investigation and Reduction of Combustion Mechanisms*, Low-temperature Combustion and Autoignition, Elsevier, Amsterdam, The Netherlands, 1997.

[17] Charrier, P. and Dubroca, B., "Asymptotic Transport Model for Heat and Mass Transfer in Reactive Porous Media," *SIAM Journal on Multiscale Modeling and Simulation*, Vol. 2, No. 1, 2003, pp. 124–157.

[18] Charrier, P., Dubroca, B., Duffa, G., Epherre, J.-F., and Preux, C., "Modeling and Computing Heat Transfer in Pyrolyzable Thermal Protection Systems," 5th European Workshop on Thermal Protection Systems and Hot Structures, Noordwijk, The Netherlands, May 2006.

[19] Curry, D. M. and Stephens, E. W., "Apollo Ablator Thermal Performance at Superorbital Entry Velocities," Tech. Rep. TN D 5969, NASA, Sept. 1970.

[20] Vignoles, G., Coindreau, O., Ahmadi, A., and Bernard, D., "Assessment of Structural and Transport Properties in Fibrous C/C Composite Preforms as Digitized by X-ray CMT. Part II : Heat and Gas Transport," *Journal of Materials Research*, Vol. 22, No. 6, 2007, pp. 1537–1550.

[21] Pike, R. W., Del Valle, E. G., and April, G. C., "Non-Equilibrium Flow and the Kinetics of Chemical Reactions in the Char Zone," Tech. Rep. NASA RFL-7, Reacting Fluid Laboratory, Louisiana State University, July 1967.

[22] Vignoles, G., *Reactive Processes in High Temperature Porous Materials*, Porous Media Interaction with High Temperature and High Speed Flows, Von Karman Institute for Fluid Dynamics, Rhode Saint Genese, Belgium, 2015.

[23] Selvaduray, G. and Cox, M., "1997-1998 Annual Report Thermal Protection Materials Development," Tech. Rep. CR 208331, NASA, 1998.

[24] Marschall, J. and Milos, F. S., "Gas Permeability of Rigid Fibrous Refractory Insulations," *Journal of Thermophysics and Heat Transfer*, Vol. 12, No. 4, Oct. 1998, pp. 528–535.

[25] White, S., "Solar Tower Radiation Testing of Phenolic Impregnated Carbon," *Journal of Spacecraft and Rockets*, Vol. 49, No. 5, Sept. 2012, pp. 889–893.

[26] Quintard, M., *Introduction to Heat and Mass Transport in Porous Media*, Porous Media Interaction with High Temperature and High Speed Flows, Von Karman Institude for Fluid Dynamics, Rhode Saint Genese, Belgium, 2015.

[27] Engelke, W. T., Pyron, C. M., and Pears, C. D., "Thermal and Mechanical Properties of a Nondegraded and Thermally Degraded Phenolic Carbon Composite," Tech. Rep. NASA CR-896, Southern Research Institute, Oct. 1967.

[28] Florio, J., Henderson, J. B., Test, F. L., and Hariharan, R., "Characterization of Forced Convection Heat Transfer in Decomposing, Glass-Filled Polymer Composites," *Journal of Composite Materials*, Vol. 25, Nov. 1991, pp. 1515–1539.

[29] Florio, J., Henderson, J. B., Test, F. L., and Hariharan, R., "A Study of the Effects of the Assumption of Local-Thermal Equilibrium on the Overall Thermally-Induced Response of a Decomposing, Glass-filled Polymer Composite," *International Journal of Heat and Mass Transfer*, Vol. 34, No. 1, 1991, pp. 135–147.

[30] Alazmi, B. and Vafai, K., "Analysis of Fluid Flow and Heat Transfer Interfacial Conditions between a Porous Medium and a Fluid Layer," *International Journal of Heat and Mass Transfer*, Vol. 44, No. 9, May 2001, pp. 1735–1749.

[31] Weng, H., Bailey, S. C. C., and Martin, A., "Numerical study of iso-Q sample geometric effects on charring ablative materials," *International Journal of Heat and Mass Transfer*, Vol. 80, No. 5, Jan. 2015, pp. 570–596.

[32] Tran, H. K., Johnson, C. E., Rasky, D. J., Hui, F. C. L., Hsu, M., Chen, T., Chen, Y. K., Paragas, D., and Koyabachi, L., "Phenolic Impregnated Carbon Ablators (PICA) as Thermal Protection Systems for Discovery Missions," Tech. Rep. 110440, NASA, April 1997.

[33] Zhao, C. Y., Lun, T. J., and Hodson, H. P., "Thermal Radiation in Ultralight Metal Foams with Open Cells," *International Journal of Heat and Mass Transfer*, Vol. 47, No. 2, 2004, pp. 2927–2939.

[34] Taine, J., *Introduction to Heat and Mass Transport in Porous Media*, Statistical Characterization of Radiative Properties of Homogeneous, Anisotropic and Non-Homogeneous Porous Media, Von Karman Institude for Fluid Dynamics, Rhode Saint Genese, Belgium, 2015.